Article

Preindustrial $^{14}CH_4$ indicates greater anthropogenic fossil CH_4 emissions

https://doi.org/10.1038/s41586-020-1991-8

Received: 27 May 2019

Accepted: 27 November 2019

Published online: 19 February 2020

Check for updates

Benjamin Hmiel[1]✉, V. V. Petrenko[1], M. N. Dyonisius[1], C. Buizert[2], A. M. Smith[3], P. F. Place[1], C. Harth[4], R. Beaudette[4], Q. Hua[3], B. Yang[3], I. Vimont[5], S. E. Michel[6], J. P. Severinghaus[4], D. Etheridge[7], T. Bromley[8], J. Schmitt[9], X. Faïn[10], R. F. Weiss[4] & E. Dlugokencky[11]

Atmospheric methane (CH_4) is a potent greenhouse gas, and its mole fraction has more than doubled since the preindustrial era[1]. Fossil fuel extraction and use are among the largest anthropogenic sources of CH_4 emissions, but the precise magnitude of these contributions is a subject of debate[2,3]. Carbon-14 in CH_4 ($^{14}CH_4$) can be used to distinguish between fossil (^{14}C-free) CH_4 emissions and contemporaneous biogenic sources; however, poorly constrained direct $^{14}CH_4$ emissions from nuclear reactors have complicated this approach since the middle of the 20th century[4,5]. Moreover, the partitioning of total fossil CH_4 emissions (presently 172 to 195 teragrams CH_4 per year)[2,3] between anthropogenic and natural geological sources (such as seeps and mud volcanoes) is under debate; emission inventories suggest that the latter account for about 40 to 60 teragrams CH_4 per year[6,7]. Geological emissions were less than 15.4 teragrams CH_4 per year at the end of the Pleistocene, about 11,600 years ago[8], but that period is an imperfect analogue for present-day emissions owing to the large terrestrial ice sheet cover, lower sea level and extensive permafrost. Here we use preindustrial-era ice core $^{14}CH_4$ measurements to show that natural geological CH_4 emissions to the atmosphere were about 1.6 teragrams CH_4 per year, with a maximum of 5.4 teragrams CH_4 per year (95 per cent confidence limit)—an order of magnitude lower than the currently used estimates. This result indicates that anthropogenic fossil CH_4 emissions are underestimated by about 38 to 58 teragrams CH_4 per year, or about 25 to 40 per cent of recent estimates. Our record highlights the human impact on the atmosphere and climate, provides a firm target for inventories of the global CH_4 budget, and will help to inform strategies for targeted emission reductions[9,10].

Atmospheric measurements of carbon-13 in methane ($\delta^{13}CH_4$) have been used to estimate the fossil fraction of the contemporaneous CH_4 budget[3]. This approach relies on having accurate estimates of the $\delta^{13}C$ signatures of the major CH_4 source categories (fossil, microbial and biomass burning) and the strength of the biomass burning source. Large uncertainties in these parameters in the past preclude accurate $\delta^{13}CH_4$-based estimates of preindustrial-era fossil CH_4 emissions[8,11,12]. Radiocarbon (^{14}C) is an ideal tracer for quantifying the fossil component of the atmospheric CH_4 budget because all ^{14}C in fossil CH_4 has decayed. By contrast, biogenic CH_4 sources (wetlands, biomass burning) have a ^{14}C activity similar to that of contemporaneous atmospheric CO_2 (ref. [4,8]). Interpretation of atmospheric $^{14}CH_4$ measurements from 1987–2000 suggests that the fossil fraction of the contemporary CH_4 budget is $30 \pm 2.3\%$ (ref. [13]; 1σ). However, the interpretation of atmospheric $^{14}CH_4$ in recent decades has been complicated by (1) rapidly changing atmospheric $^{14}CO_2$ (from above-ground nuclear testing and fossil fuel emissions) that propagates into biospheric CH_4 emissions[13], and (2) direct $^{14}CH_4$ emissions from nuclear power plants[4,5]. By contrast, palaeoatmospheric $^{14}CH_4$ measurements from ice cores offer a direct constraint on natural geological CH_4 emissions without these complications. Whereas geological CH_4 emissions have the potential to change on tectonic- and glacial-cycle timescales[14], they have very probably been constant over the past few centuries. The preindustrial-era emission estimates can therefore be applied to the modern CH_4 budget with confidence.

Ice core $^{14}CH_4$ analysis is challenging owing to both the very large sample requirement (~1,000 kg of ice) and interference from in situ

[1]Department of Earth and Environmental Sciences, University of Rochester (UR), Rochester, NY, USA. [2]College of Earth, Ocean and Atmospheric Sciences, Oregon State University (OSU), Corvallis, OR, USA. [3]Australian Nuclear Science and Technology Organisation (ANSTO), Lucas Heights, New South Wales, Australia. [4]Scripps Institution of Oceanography (SIO), University of California San Diego, La Jolla, CA, USA. [5]Cooperative Institute for Research in Environmental Sciences (CIRES), University of Colorado and National Oceanic and Atmospheric Administration (NOAA) Global Monitoring Division (GMD), Boulder, CO, USA. [6]Institute of Arctic and Alpine Research (INSTAAR), University of Colorado, Boulder, CO, USA. [7]Climate Science Centre, Commonwealth Scientific and Industrial Research Organisation (CSIRO) Oceans and Atmosphere, Aspendale, Victoria, Australia. [8]National Institute of Water and Atmospheric Research (NIWA), Wellington, New Zealand. [9]Climate and Environmental Physics, Physics Institute and Oeschger Centre for Climate Change Research, University of Bern, Bern, Switzerland. [10]University of Grenoble Alpes, CNRS, IRD, Grenoble INP, Institut des Géosciences de l'Environnement (IGE), Grenoble, France. [11]NOAA, Earth System Research Laboratory (ESRL), Boulder, CO, USA. ✉e-mail: bhmiel@ur.rochester.edu

cosmogenic ^{14}C production within the ice crystal lattice[15]. We address the former by using a large-diameter ice drill and a large-volume ice-melting apparatus (Supplementary Information section 1) to obtain sufficient CH_4 (~20 μg C) for ^{14}C analysis by accelerator mass spectrometry. To address the latter, we follow the established[8,16] approach of analysing ^{14}C of carbon monoxide (CO) in parallel with $^{14}CH_4$. ^{14}CO is very sensitive to in situ cosmogenic ^{14}C production[15] and can be used to precisely establish the effective cosmic ray exposure history of each sample. We then correct the $^{14}CH_4$ data using the known in situ cosmogenic $^{14}CH_4/^{14}CO$ production ratio in ice[15] (Supplementary Information sections 5, 6). The in situ cosmogenic $^{14}CH_4$ component in the samples used in this study is much lower (<2% of total $^{14}CH_4$) than in ablation-zone ice used in previous palaeoatmospheric $^{14}CH_4$ studies (~30% of total $^{14}CH_4$)[8,16]. We present new $^{14}CH_4$ data from large-volume ice core samples and firn air sampling from Summit, Greenland, which we combine with prior firn air $^{14}CH_4$ measurements from Law Dome DSSW20K[4] and Megadunes[17], Antarctica. Our combined record spans from about 1750 to 2013 and captures the evolution of atmospheric $^{14}CH_4$ since the preindustrial era (Fig. 1). The movement of gases within the firn and closure into bubbles is characterized using a firn air transport model[18], and the time series of atmospheric $^{14}CH_4$ is reconstructed using a matrix inversion technique[19,20] (Supplementary Information section 9).

Our atmospheric $^{14}CH_4$ reconstruction (Fig. 1) is indistinguishable from the $^{14}CO_2$-derived contemporaneous biogenic $^{14}CH_4$ signature (blue curve, Supplementary Information section 10) before 1880, suggesting very low natural geological CH_4 emissions. Atmospheric $^{14}CH_4$ began to decrease around 1880, coincident with substantial increases in the use of coal, oil and natural gas (Fig. 2)[21]. The precise timing of the $^{14}CH_4$ minimum (in the 1940s in our reconstruction) is difficult to establish owing to the broad age distributions of individual firn air and ice core samples, as well as the smoothing applied by the matrix inversion technique to address the non-uniqueness of the solution[19]. Beyond this fossil ^{14}C minimum, our samples are affected by the propagation of ^{14}C from atmospheric nuclear testing into the carbon cycle[22] and by emissions from nuclear power plants (starting in the 1970s), which drove a sustained $^{14}CH_4$ increase despite decreasing $^{14}CO_2$[4,5]. We calculate the fossil CH_4 fraction and develop a time series of fossil CH_4 emissions (Fig. 2) using a one-box atmospheric model (Supplementary Information section 10). The broad age distributions of our air samples (Supplementary Fig. 3) result in a smoothed representation of the atmospheric $^{14}CH_4$ history that cannot capture the abrupt increase of bomb $^{14}CO_2$ (and subsequently $^{14}CH_4$) starting in 1955. Therefore, we interpret the fossil CH_4 fraction only before the 1940s. We find an increase in the total (geological plus anthropogenic) fossil emissions from negligible CH_4 emissions in the mid-19th century to 64.8 teragrams CH_4 per year (Tg CH_4 yr^{-1}) in 1940.

Assuming that the oldest ice core $^{14}CH_4$ sample in our reconstruction (mean age 1756 AD; Fig. 1) is devoid of anthropogenic fossil CH_4 contributions, we use the contemporaneous biogenic $^{14}CH_4$ source signature to calculate the natural geological CH_4 emissions during the preindustrial era: 1.6 Tg CH_4 yr^{-1} with a 95% confidence interval (CI) maximum of 5.4 Tg CH_4 yr^{-1} (Supplementary Information section 10, Supplementary Fig. 5). Our 95% confidence limit of 5.4 Tg CH_4 yr^{-1} agrees well with, and provides a tighter constraint than, the only other published $^{14}CH_4$-based estimate of natural geological CH_4 emissions from ice cores, which sampled air from the most recent deglaciation (0 to 15.4 Tg CH_4 yr^{-1}, 95% CI range)[8].

Our result is much lower than estimates from recent source inventory ('bottom-up') studies typically used in global CH_4 budgets[2], which suggest natural geological emissions of ~40–60 Tg CH_4 yr^{-1} (ref. [6]). A recent study[7] aimed at developing gridded maps of geological CH_4 emissions revised this estimate downwards to 37 Tg CH_4 yr^{-1} on the basis of data and modelling specifically targeted for gridding; however, the CH_4 emissions increased to 43–50 Tg CH_4 yr^{-1} when extrapolated to account for temporal variability in mud volcano eruptions and onshore or submarine geological seeps that lack location-specific measurements. Natural fossil CH_4 emissions of about 40 Tg CH_4 yr^{-1} (out of total preindustrial-era CH_4 emissions of 215 Tg CH_4 yr^{-1}; Supplementary Fig. 5) would result in a preindustrial-era $\Delta^{14}CH_4$ of around −185‰, which is in clear disagreement with our data (1.5‰ ± 21.2‰, 2σ; Fig. 1). Bringing our ^{14}C results into agreement with the bottom-up estimates of natural fossil CH_4 emissions would require an order-of-magnitude larger correction for in situ cosmogenic $^{14}CH_4$. This would in turn require either an order-of-magnitude higher ^{14}CO content in the sampled ice or an order-of-magnitude higher in situ $^{14}CH_4/^{14}CO$ production ratio; both of these possibilities are well outside the respective uncertainties. The added uncertainties arising from the in situ and procedural corrections to the measured $^{14}CH_4$ are also too small to explain the disagreement

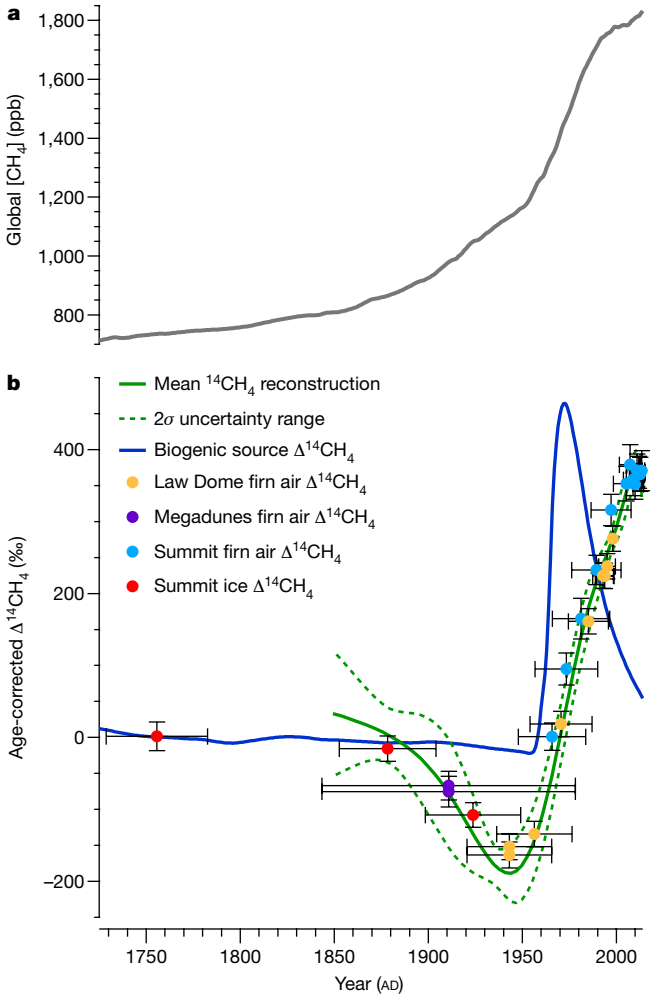

Fig. 1 | Reconstruction of atmospheric $^{14}CH_4$ from firn air and ice core data. **a**, Global CH_4 mole fraction, [CH_4], reconstructed from ice core, firn air and atmospheric measurements[1]. ppb, parts per billion. **b**, Reconstructed history of atmospheric $\Delta^{14}CH_4$ from firn air and ice core samples (this study). Dotted lines represent the 95% confidence range based on all calculated $^{14}CH_4$ histories using three different inversion methods (Supplementary Information section 9). Ice core and firn air $\Delta^{14}CH_4$ measurements are shown at the mean age of the modelled air age distribution. Vertical error bars on the $\Delta^{14}CH_4$ data from each site represent the 2σ uncertainty for each sample after corrections (Supplementary Information Tables 2, 6), and horizontal error bars represent ±2Δ, where Δ is the spectral width of the sample-air age distribution[20]. We also plot the $^{14}CH_4$ signature of the contemporaneous biogenic source (blue; Supplementary Information section 10). Our time series begins in 1850 because the age distributions of the collected ice core samples have poor coverage of air from ~1780 to 1850 (Supplementary Information section 10, Supplementary Fig. 3B).

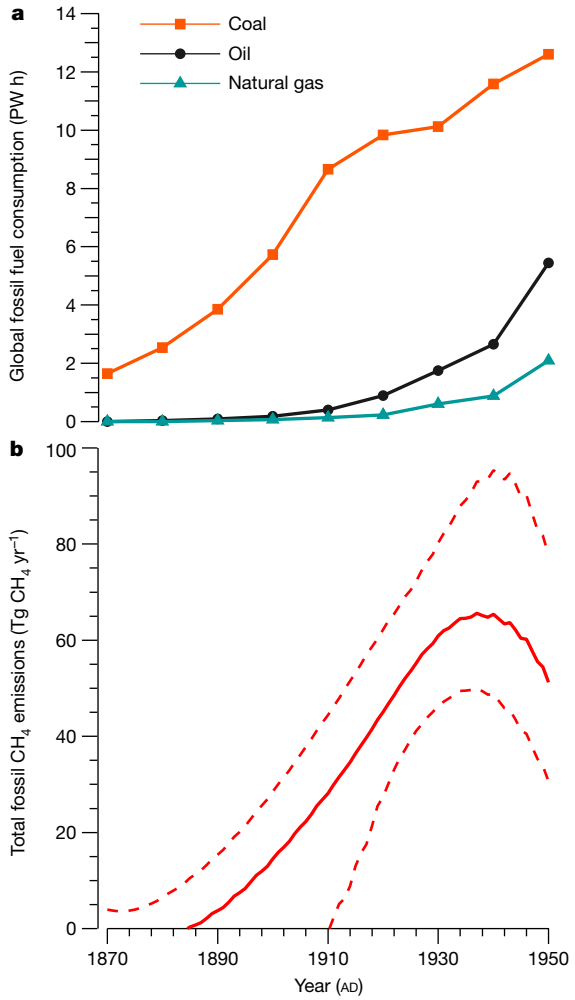

Fig. 2 | Growth in fossil CH_4 emissions and fossil fuel consumption. **a**, Historical fossil fuel energy consumption[21]. **b**, Calculated total fossil CH_4 emission history (solid line) from the one-box model (Supplementary Information section 10). The dashed lines show the 95% confidence interval.

(Supplementary Information section 10, Supplementary Information Table 8).

Diffuse microseepage (24 Tg CH_4 yr^{-1}), macro-seeps and mud volcanoes (8.1 Tg CH_4 yr^{-1}), submarine seepage (>7 Tg CH_4 yr^{-1}) and geothermal manifestations (5.7 Tg CH_4 yr^{-1}) represent the main categories of natural geological CH_4 emissions in the latest comprehensive bottom-up analysis[7]. Each of these four categories is nearly equivalent to, or exceeds, our upper bound (at 95% confidence) on the total preindustrial-era geological CH_4 emissions (5.4 Tg CH_4 yr^{-1}). Emission estimates for diffuse microseepage are based on limited flux-chamber measurements in regions of known gas seepage (for example, ref. [23]), which are scaled up to a global flux estimate based on the total dryland area situated above hydrocarbon reservoirs (~10% of Earth's total land surface area), the percentage of measurements that show a positive flux, and emission rates chosen on the basis of several geological factors[7]. It is possible that the uncertainties associated with such global upscaling are much larger than reported, resulting in an overestimation by an order of magnitude or more. Similarly, emission estimates from macro-seeps, mud volcanoes and geothermal manifestations are derived from limited observations, which are scaled up to a global total[7]. To provide a sense of scale for the extrapolation in the case of mud volcanoes, ~0.0026 Tg CH_4 yr^{-1} of measured CH_4 emissions (table S2 in the supplement of ref. [7]) are scaled up to 6.1 Tg CH_4 yr^{-1} (table 2 in ref. [7]).

With regard to submarine seepage, recent studies suggest that CH_4 emissions to the atmosphere are probably very low owing to rapid dissolution of rising bubbles[24] and rapid oxidation of dissolved CH_4 (ref. [25]). Furthermore, $^{14}CH_4$ measurements in surface waters indicate minimal quantities of fossil CH_4 even in shallow waters over areas of active seeps or methane hydrate degradation[26]. Our atmospheric $^{14}CH_4$ measurements for the preindustrial era indicate that either (1) the uncertainties associated with global upscaling of geological emissions from discrete measurements result in overestimation by an order of magnitude, or (2) geological CH_4 emissions quantified by these measurements were not present in the preindustrial era and may have been triggered by fossil fuel extraction from hydrocarbon reservoirs or other anthropogenic activity such as groundwater aquifer depletion. If the latter is true, such emissions cannot be considered natural.

A recent study[3] used ice core $\delta^{13}CH_4$ measurements to arrive at a natural geological CH_4 emission estimate that is on par with what is indicated by bottom-up methods (~50 Tg CH_4 yr^{-1}). However, ref. [8] showed that ice core $\delta^{13}CH_4$ data do not provide a strong constraint on preindustrial-era geological emissions and are also compatible with a minimal geological source. Measurements of ethane[27] in ice cores have also been used to suggest considerable emissions of fossil CH_4 during the preindustrial era. However, this is also an ambiguous constraint because ice core measurements of ethane mole fraction cannot discriminate between contributions from biomass burning (a major source) and natural geological emissions[11]. Our preindustrial-era $^{14}CH_4$ measurements, by contrast, place an unambiguous constraint on natural fossil CH_4 emissions by directly recording the ^{14}C-free fraction of atmospheric CH_4.

Our $^{14}CH_4$ reconstruction does not allow accurate quantification of the post-1950 fossil CH_4 budget, owing to relatively poor constraints on the interfering nuclear $^{14}CH_4$ sources. Previous work used atmospheric $\delta^{13}CH_4$ measurements to quantify the global fossil CH_4 source in recent decades[3], but relied on inventory-based assessments to constrain the natural geological component. We combine our $^{14}CH_4$-based constraint on natural geological emissions (1.6 Tg CH_4 yr^{-1}) with $\delta^{13}CH_4$-based constraints on the total fossil source (following the same one-box model approach as ref. [3]; Supplementary Information section 11) to estimate recent anthropogenic fossil CH_4 emissions. This approach yields 177 ± 37 Tg CH_4 yr^{-1} (1σ) for anthropogenic fossil CH_4 emissions during 2003–2012. Our estimate is 22% higher than the previous estimate of 145 ± 23 Tg CH_4 yr^{-1} (1σ) over the same interval[3], and 33–55% higher than the range of bottom-up estimates (114–133 Tg CH_4 yr^{-1}; ref. [2]). We note that our $\delta^{13}CH_4$-based calculation uses an updated value for the CH_4 sink isotopic fractionation (Supplementary Information section 11); if we use the same value as ref. [3], the anthropogenic fossil source estimate is 194 ± 34 Tg CH_4 yr^{-1} for the same time period.

Our results indicate that bottom-up inventories strongly underestimate CH_4 emissions from fossil fuel extraction, distribution and use. A study using both ground-based facility-scale measurements and verification from aircraft sampling found that US oil and natural-gas CH_4 emissions (largely from the production and gathering industry segments) are ~60% higher than those reported by the US Environmental Protection Agency[28], one of the primary data sources used in bottom-up inventories[2]. If we consider a scenario in which the global bottom-up emissions of fossil CH_4 from the oil and natural-gas industries (79 Tg CH_4 yr^{-1}; ref. [2]) are similarly underreported by 60%, this would amount to unreported emissions of ~47 Tg CH_4 yr^{-1}, which is in agreement with the fossil CH_4 emission shortfall that we identify in the current generation of bottom-up inventories (44–63 Tg CH_4 yr^{-1}). Our results imply that anthropogenic fossil CH_4 emissions now account for about 30% of the global CH_4 source and for nearly half of anthropogenic emissions, highlighting the critical role of emission reductions in mitigating climate change[9,10].

Online content

Any methods, additional references, Nature Research reporting summaries, source data, extended data, supplementary information, acknowledgements, peer review information; details of author contributions and competing interests; and statements of data and code availability are available at https://doi.org/10.1038/s41586-020-1991-8.

1. Meinshausen, M. et al. Historical greenhouse gas concentrations for climate modelling (CMIP6). *Geosci. Model Dev.* **10**, 2057–2116 (2017).
2. Saunois, M. et al. The global methane budget 2000–2012. *Earth Syst. Sci. Data* **8**, 697–751 (2016).
3. Schwietzke, S. et al. Upward revision of global fossil fuel methane emissions based on isotope database. *Nature* **538**, 88–91 (2016); corrigendum **543**, 452 (2017).
4. Lassey, K. R., Etheridge, D. M., Lowe, D. C., Smith, A. M. & Ferretti, D. F. Centennial evolution of the atmospheric methane budget: what do the carbon isotopes tell us? *Atmos. Chem. Phys.* **7**, 2119–2139 (2007).
5. Zazzeri, G., Acuña Yeomans, E. & Graven, H. D. Global and regional emissions of radiocarbon from nuclear power plants from 1972 to 2016. *Radiocarbon* **60**, 1067–1081 (2018).
6. Etiope, G. *Natural Gas Seepage: The Earth's Hydrocarbon Degassing* Vol. 1 (Springer International Publishing, 2015).
7. Etiope, G., Ciotoli, G., Schwietzke, S. & Schoell, M. Gridded maps of geological methane emissions and their isotopic signature. *Earth Syst. Sci. Data* **11**, 1–22 (2019).
8. Petrenko, V. V. et al. Minimal geological methane emissions during the Younger Dryas–Preboreal abrupt warming event. *Nature* **548**, 443–446 (2017).
9. Höglund-Isaksson, L. Global anthropogenic methane emissions 2005–2030: technical mitigation potentials and costs. *Atmos. Chem. Phys.* **12**, 9079–9096 (2012).
10. Howarth, R. W. Methane emissions and climatic warming risk from hydraulic fracturing and shale gas development: implications for policy. *Eng. Emis. Con. Tech.* **3**, 45–54 (2015).
11. Nicewonger, M. R., Aydin, M., Prather, M. J. & Saltzman, E. S. Large changes in biomass burning over the last millennium inferred from paleoatmospheric ethane in polar ice cores. *Proc. Natl Acad. Sci. USA* **115**, 12413–12418 (2018).
12. Bock, M. et al. Glacial/interglacial wetland, biomass burning, and geologic methane emissions constrained by dual stable isotopic CH_4 ice core records. *Proc. Natl Acad. Sci. USA* **114**, E5778–E5786 (2017).
13. Lassey, K. R., Lowe, D. C. & Smith, A. M. The atmospheric cycling of radiomethane and the "fossil fraction" of the methane source. *Atmos. Chem. Phys.* **7**, 2141–2149 (2007).
14. Etiope, G., Milkov, A. V. & Derbyshire, E. Did geologic emissions of methane play any role in Quaternary climate change? *Global Planet. Change* **61**, 79–88 (2008).
15. Petrenko, V. V. et al. Measurements of ^{14}C in ancient ice from Taylor Glacier, Antarctica constrain in situ cosmogenic $^{14}CH_4$ and ^{14}CO production rates. *Geochim. Cosmochim. Ac.* **177**, 62–77 (2016).
16. Petrenko, V. V. et al. $^{14}CH_4$ measurements in Greenland Ice: investigating last glacial termination CH_4 sources. *Science* **324**, 506–508 (2009).
17. Severinghaus, J. P. et al. Deep air convection in the firn at a zero-accumulation site, central Antarctica. *Earth Planet. Sci. Lett.* **293**, 359–367 (2010).
18. Buizert, C. et al. Gas transport in firn: multiple-tracer characterisation and model intercomparison for NEEM, Northern Greenland. *Atmos. Chem. Phys.* **12**, 4259–4277 (2012).
19. Rommelaere, V., Arnaud, L. & Barnola, J.-M. Reconstructing recent atmospheric trace gas concentrations from polar firn and bubbly ice data by inverse methods. *J. Geophys. Res. Atmos.* **102**, 30069–30083 (1997).
20. Trudinger, C. et al. Reconstructing atmospheric histories from measurements of air composition in firn. *J. Geophys. Res. Atmos.* **107**, (2002).
21. Smil, V. *Energy Transitions: Global and National Perspectives* (ABC-CLIO, 2016).
22. Hua, Q., Barbetti, M. & Rakowski, A. Z. Atmospheric radiocarbon for the period 1950–2010. *Radiocarbon* **55**, 2059–2072 (2013).
23. Etiope, G. & Klusman, R. W. Microseepage in drylands: flux and implications in the global atmospheric source/sink budget of methane. *Global Planet. Change* **72**, 265–274 (2010).
24. McGinnis, D. F., Greinert, J., Artemov, Y., Beaubien, S. & Wüest, A. Fate of rising methane bubbles in stratified waters: how much methane reaches the atmosphere? *J. Geophys. Res. Oceans* **111**, C09007 (2006).
25. Leonte, M. et al. Rapid rates of aerobic methane oxidation at the feather edge of gas hydrate stability in the waters of Hudson Canyon, US Atlantic Margin. *Geochim. Cosmochim. Acta* **204**, 375–387 (2017).
26. Sparrow, K. J. et al. Limited contribution of ancient methane to surface waters of the U.S. Beaufort Sea shelf. *Sci. Adv.* **4**, eaao4842 (2018).
27. Nicewonger, M. R., Verhulst, K. R., Aydin, M. & Saltzman, E. S. Preindustrial atmospheric ethane levels inferred from polar ice cores: a constraint on the geologic sources of atmospheric ethane and methane. *Geophys. Res. Lett.* **43**, 214–221 (2016).
28. Alvarez, R. A. et al. Assessment of methane emissions from the U.S. oil and gas supply chain. *Science* **361**, 186–188 (2018).

Data availability

The ice core and firn air $^{14}CH_4$ data presented in Fig. 1 are provided in Supplementary Information Tables 2, 6. Additional measurements not provided in Supplementary Information Tables 1–8 are available via the NSF Arctic Data Center at https://doi.org/10.18739/A2599Z216.

Code availability

The code for the firn air inverse model and atmospheric box model (MATLAB) is available from the corresponding author upon request.

Acknowledgements This work was supported by US NSF awards OPP-1203779 (V.V.P.) OPP-1203686, OPP-0230452, ANT-0839031 (J.P.S.) ARC-1204084, ARC-1702920 (C.B.), a Packard Fellowship for Science and Engineering (V.V.P.), the National Institute of Water and Atmospheric Research through the Greenhouse Gases, Emissions and Carbon Cycle Science Programme (T.B.) and the Australian Government for the Centre for Accelerator Science at ANSTO through the National Collaborative Research Infrastructure Strategy (A.M.S.). We thank J. McConnell and P. Vallelonga for the interpretation of the ice core CFA data; P. Neff and E. Steig for sharing the ice-thinning model code; L. Davidge, J. Edwards, M. Pacicco and A. Adolph for assistance with firn air and ice core sampling; M. Jayred, L. Albershardt, T. Kuhl, D. Kirkpatrick and the US Ice Drilling programme for ice-drilling support; K. Gorham, J. Jenkins, D. Einerson, Polar Field Services and the 109th New York Air National Guard for logistical support; the Australian Antarctic Science Program for supporting the Law Dome drilling and firn air sampling and CSIRO GASLAB, in particular R. Langenfelds, for analysis of the firn air sample trace gas concentrations.

Author contributions B.H. and V.V.P. designed the study and conducted field logistical and scientific preparations; B.H., V.V.P., M.N.D., C.B., P.F.P., R.B., J.S. and X.F. collected samples at Summit; B.H. measured [CO] and extracted CH_4 and CO from firn air and ice core samples; C.B. developed the firn modelling code; B.H. and M.N.D. developed the box-model calculations; Q.H. and B.Y. graphitized the ^{14}C samples; A.M.S. measured ^{14}C; P.F.P. and I.V. measured $\delta^{13}CO$; S.E.M. measured $\delta^{13}CH_4$; C.H. measured [CH_4] and halogenated trace gases under the supervision of R.F.W.; E.D. supervised the firn air trace gas measurements; J.P.S. measured $\delta Xe/Kr$, $\delta Kr/N_2$, $\delta Xe/N_2$ and $\delta Ne/N_2$ and collected Megadunes firn air samples; R.B. measured the $\delta^{15}N$ of N_2, the $\delta^{18}O$ of O_2, $\delta O_2/N_2$ and $\delta Ar/N_2$; D.E. collected and supervised the analyses of the Law Dome firn air samples; T.B. extracted CH_4 from Megadunes and Law Dome samples; B.H. and V.V.P. analysed the data and B.H. drafted the manuscript with contribution from all authors.

Competing interests The authors declare no competing interests.

Additional information
Supplementary information is available for this paper at https://doi.org/10.1038/s41586-020-1991-8.
Correspondence and requests for materials should be addressed to B.H.
Reprints and permissions information is available at http://www.nature.com/reprints.